H_2GO: WATER-POWERED CART

B. Ho, J. Jacobowitz, J. Yoon, N. Shlayan, D. Wootton

The Cooper Union Albert Nerken School of Engineering, New York, NY

ABSTRACT

This year's ASME Student Design Competition, titled "H_2Go", challenged students to design a water-powered, remote-controlled transportation device. Teams were tasked with implementing a method of converting the potential energy of water into useful energy to drive the device across the playing field, transporting as much water as possible within the given time limit. Points were awarded based on the quantity of water transported, with bonus multipliers for performing extra tasks or for having a highly-rated design. To generate electrical energy, we manufactured a custom alternator from 3D-printed parts, neodymium magnets, and magnet wire. To spin our alternator, we directed a jet of water at a 3D-printed Pelton turbine. The energy was stored in a supercapacitor bank and was used to power two low-voltage DC motors when controlled by an Arduino Bluetooth-connected smartphone app. The design cycle focused on refinement, resulting in improvements such as tripling the drive distance through redesigning the motor controllers and altering the flow system to reduce the charging time by 48 percent. The design scored 2^{nd} out of 17 in the competition.

1 INTRODUCTION

1.1 Project Significance

Interests in renewable energy application have been on the rise to tackle climate change. Revisiting the 2011 ASME Student Design Competition's (SDC) theme, the goal of the 2022 ASME SDC H_2Go competition was to use the potential energy of water as an energy source to propel a cart and transport the water. Quoting the 2011 competition rules, "Devices to convert and store this energy could be created and an untapped and readily available energy source utilized. In addition, the water itself could be stored for a variety of everyday uses."[1] This project is a proof-of-concept for an efficient water energy conversion method.

The project is multidisciplinary in nature, consisting of aspects of electrical circuits, thermodynamics, fluids, dynamics, mechanics of materials (and stress and applied elasticity), and mechatronics, therefore, it requires a multidisciplinary team of mechanical and electrical engineering students. The competition brought engineering students to tackle current issues on climate change through a process brought out the creativity and ingenuity of the students while also being fun.

2 COMPETITION OVERVIEW

The premise of the competition is based on *efficiently* converting and using energy. Each team needs to design and build a remote-controlled water-powered device that will be used to transport water from one corner of the $3m \times 3m$ playing field (Figure 1a) to the opposite corner within the time limit of the competition. Points are awarded based on the amount of water transported, where more water transported means more points. The catch is that all the propulsion energy must be generated through the conversion of the water's energy (i.e. potential energy) to some some usable form of energy.

2.1 Problem Statement

Design a small, remote-controlled, water-powered device for the 2022 ASME Student Design Competition that can transport as much water as possible across the competition playing field within the given time limit.

3 DESIGN REQUIREMENTS

3.1 Design Constraints

The competition rules outlined three main design constraints.[1]

1. **Remote controlled**: The device must be remote controlled, such as through radio control, and operated by, at most, a single team member.

2. **Size**: The device must fit within a $50cm \times 50cm \times 50cm$ rigid, lidded box

3. **Initial charge**: The device must start the competition without any initially stored propulsion energy (auxiliary electronics may run on a battery that is charged at the start of the competition, see general rule 6 [1]). If the propulsion system of the remote controlled car is powered by a battery, the battery must start empty.

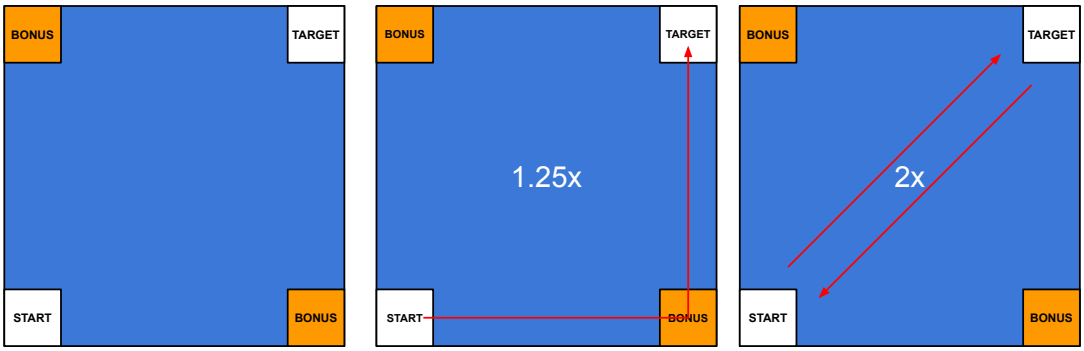

(a) Playing field **(b)** Target Bonus **(c)** Return Bonus

FIGURE 1: (a) Scaled drawing of the competition playing field. The entire playing field is $3m \times 3m$ with the start, target, and bonus areas all $0.5m \times 0.5m$. (b) Possible path to follow for the 1.25x target bonus multiplier. (c) Possible path to follow for the 2x return bonus multiplier.

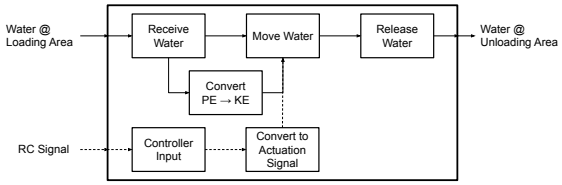

FIGURE 2: A functional requirements diagram outlining the necessary functions of the device without detailing how they will be implemented.

3.2 Functional Requirements

A function requirements diagram (Figure 2) details all the requirements necessary for the device to complete in the competition without going into detail as to *how* it will be implemented. This simplifies the concept of the system, distilling it down to the bare minimum of what it needs to do. In essence, the system needs to be able to accept water, convert the water to usable energy, be controlled to drive to the unloading zone, and unload that water.

3.3 Design Criteria

The competition rules outline the scoring metric based on achievement and design.[1] Each round was scored based on the volume of water transported (in mL) times a bonus multiplier, Eq. (1).

$$\text{Trip Score} = \text{BONUS} \times V_{water} \tag{1}$$

The bonus multiplier was a composite of the design scoring factor, a target bonus, and a return bonus, Eq. (2).

$$\text{BONUS} = \text{Design Scoring Factor} \times \text{Target Bonus} \times \text{Return Bonus} \tag{2}$$

The design scoring factor was calculated, Eq. (3), from the judge's design score, a value from 0.0 to 10.0, based on the optional design overview video submitted two weeks before the main competition.

$$\text{Design Scoring Factor} = 1 + \frac{\text{Judge's Score}}{10} \tag{3}$$

If the device passed through a bonus area during a round, such as by following the path in Figure 1b, a $1.25\times$ multiplier was included in that trip score. If the device returned to the loading area using the remaining stored energy, such as by following the path in Figure 1c, then a $2\times$ multiplier was included in the trip score.

The total competition score was the sum of scores from each of the N rounds completed within the competition time limit, Eq. (4).

$$\text{Total Score} = \sum_{i=1}^{N} (\text{Trip Score})_i \tag{4}$$

4 DESIGN

4.1 Design Options

Two energy conversion methods were considered for the final design, an electrical version and a mechanical version. The electrical design would make use of Faraday's law, $\epsilon = -N\frac{\mathrm{d}\Phi}{\mathrm{d}t}$, which says that a time-varying magnetic flux, $\mathrm{d}\Phi/\mathrm{d}t$, passing through a coil of wire with N turns induces voltage, ϵ. The energy would be stored as electrical energy (in a battery or supercapacitor). The mechanical design would make use of a flywheel, which can store energy with its inertia (see the *Mechanical Design* appendix for more).

To decide, we created a list of pros and cons of each option, as shown in Figure 3. Compared to the mechanical option, the electrical design would be much lighter (flywheels need to be heavy to have a lot of inertia). Using electricity is also a more "modern" solution to the problem at hand, but if batteries are used, they need to

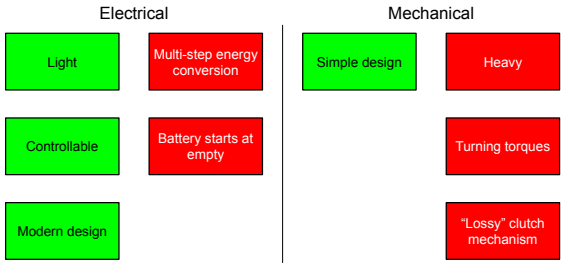

FIGURE 3: Pros and cons list for the electrical and mechanical design options.

start empty, which is unhealthy for them. The electrical design also involves a multi-step energy conversion process, making it prone to efficiency losses. The mechanical design would be simple, with fewer parts, but the angular momentum of the flywheel would make it difficult to turn (due to the conservation of angular momentum), while the electrical design would have independently controlled motors. Calculations also showed that the clutch mechanism necessary for transferring energy would be very inefficient.

Ultimately, we decided to go with the electrical design because the pros of that design outweighed the cons and because we saw a clearer path forward with that design.

4.2 Design Methodology

We aimed to design our device so we could easily replace broken parts or swap in improved versions as we iterate through the design process. To do this, we designed modular parts that could be 3D printed and were assembled using the same hardware. We also wanted to make testing an important part of the design so we could make informed design decisions. So, the device was designed through **empirical verification** and it was also designed to be **upgradeable** and **serviceable**.

4.3 Alternator

An alternator is a device that produces AC power through Faraday's law. The alternator for this project was an axial flux alternator, where the two parts of the alternator, the rotor (see *Rotor*) and stator (see *Stator*), were mounted co-axially.

4.3.1 Rotor

The rotor, shown in Figure 5c, is the moving portion of the alternator. Mounted radially around the rotor were neodymium magnets. We chose to use a specific magnet arrangement called a Halbach array, as shown in Figure 4, which consists of magnets rotated 90° from each position, creating a magnetic field that is stronger on one side. We also had mounting holes on the rotor to

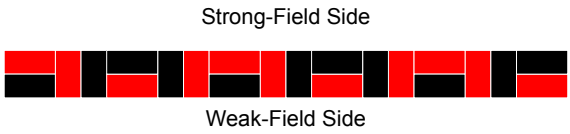

FIGURE 4: The Halbach array arrangement consists of magnets rotated 90 degrees between positions to create an asymmetric magnetic field.

allow for connected parts to be swapped out (meeting our upgradeable and serviceable goals).

The rotor went through three main design iterations, which are shown in Figure 5. The first design, Figure 5a, had a lot of of extra 3D-printed material and did not have mounting holes using the standard bolts found in most of the other parts. The second version, Figure 5b, was slimmed down and used the standard bolts for mounting, but the magnets were not strong enough. The third, and final version, Figure 5c, used stronger magnets to induce more voltage.

4.3.2 Stator

The stator, shown in Figure 6c, is the *stat*ionary portion of the alternator. Mounted radially around the stator were six tightly-wrapped coils of 28 AWG (American wire gauge) magnet wire. We connected opposite coils because they were always in phase with each other (because the coil-to-magnet ratio was 3:4), resulting in 3-phase AC power. The coil design was optimized for power (see the *Stator Optimization* appendix section for an indepth explanation).

Like the rotor, the stator also went through three main design iterations, which are shown in Figure 6. The first design, Figure 6a, was sub-optimal and did not make good use of the available space. The second version, Figure 6b, used the optimized coil design, but the coils were wrapped using a hand-drill and were not tight enough. The third, and final, version, Figure 6c, had tighter coils that were wrapped on the lathe with an improved 3D-printed tool, as shown in Figure 7.

4.3.3 Pelton Turbine

A Pelton turbine is an impulse turbine which converts translational kinetic energy of water to the angular kinetic energy of the water wheel.[2] Each blade is designed as a double bucket, which can be seen in Figure 8a, splitting the flow and redirecting it nearly 180°. Through the redirection of the flow, the Pelton turbine is able to extract more power from the water than a flat blade design. These turbines can be very efficient, reaching efficiencies of greater than 90 percent.[3]

Designing an efficient Pelton turbine requires complicated and time-consuming simulations, which were not

(a) Version 1 **(b)** Version 2 **(c)** Version 3

FIGURE 5: The 3 design iterations from (a) the original with thick walls to (b) a thinner version but with weak magnets and finally (c) with stronger magnets.

(a) Version 1 **(b)** Version 2 **(c)** Version 3

FIGURE 6: The 3 design iterations from (a) the original did not have optimized coil geometry (b) the coils were not tight and didn't fill the entire space available and finally (c) tighter coils were made closer to the designed specifications.

practical for this project. Therefore, multiple versions were 3D printed (see Figure 8b) and tested. Some designs were to small (in diameter) and did not produce enough torque to spin the electrically-loaded alternator, or were too large, producing more torque than necessary while not having a high enough angular velocity. The best one had a $4.5\,in$ diameter.

4.3.4 Alternator Assembly

Using the 3-hole pattern on the Pelton turbine and the rotor, the two were bolted together (with standoffs for space). When the Pelton turbine was hit by the jet of water, both the turbine and rotor spun. The turbine and rotor were mounted on the same shaft that passed through the stator. The stator was bolted to the side of the container (with wires passed through holes in the container wall). The assembled alternator, seen in Figure 8c, was mounted in the container to prevent splashing of water. A rectangular hole in the container, seen in Figure 9, was where the hose was held and allowed access for assembly and repairs.

4.4 Electronics

A block diagram of the electronics system in Figure 10 outlines the process of harnessing, storing, and using the electrical power. First, the alternator generates 3-phase (3ϕ) AC power. This needs to be rectified to DC power to charge the supercapacitors. Once charged, the supercapcitors can be used by sending the power through power electronics and the motor controllers to ultimately power the motor.

4.4.1 Rectifier

Figure 11 shows the full bridge rectifier circuit used to turn the AC power into DC. As mentioned, the 6 coils were connected in pairs, each of which had its own 4-diode rectifier arrangement. Typical silicon diodes have a high forward voltage drop, so Schottky diodes were used instead. The rectified voltages were combined in

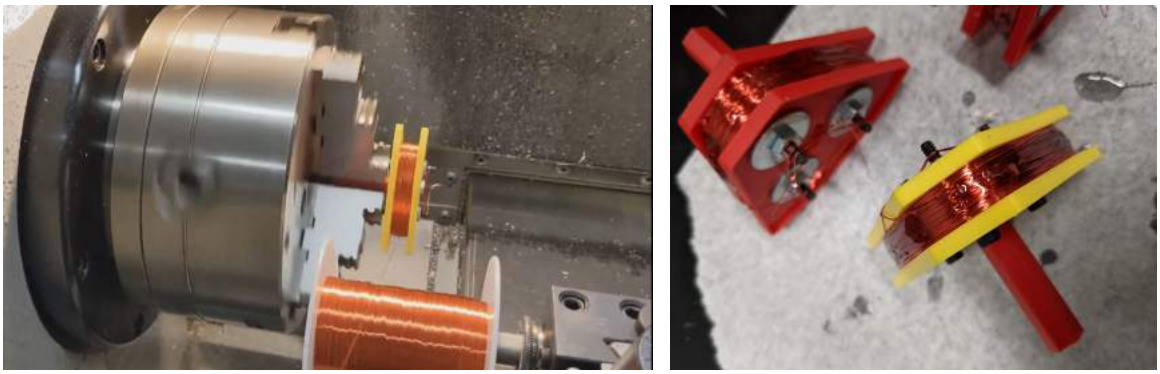

(a) Wrapping the Coil on the Lathe **(b)** Wrapped Coils in the Tools

FIGURE 7: (a) The coils were wrapped on the CNC lathe with the spool of wire mounted on a boring bar while I held tension on the line. (a) Wrapped coils were glued to prevent them from unwrapping. The plastic core of the tool was kept but the stem was broken and the sandwich plates removed.

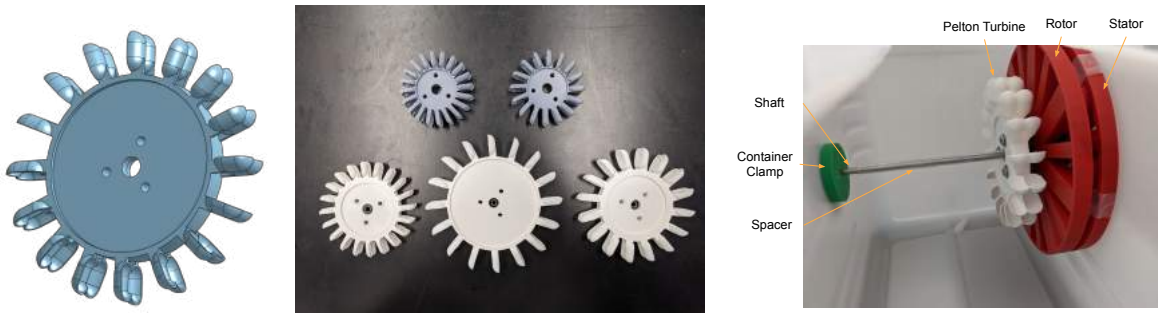

(a) Turbine 3D CAD **(b)** Turbine Iterations **(c)** Assembled Alternator

FIGURE 8: (a) 3D CAD model of the Pelton turbine showing the characteristic double-scooped buckets. The 3-bolt mounting design was used to connect it to the rotor. (b) Some Pelton versions explored for the project. The bottom right turbine was the one that was used. (c) Assembled alternator mounted on the shaft inside the container.

parallel and used to charged the supercapacitors.

4.4.2 Supercapacitors

Supercapacitors were the electrical storage unit of choice due to their ability to charge and discharge quickly, and relatively simple charging circuitry. Batteries, the other logical choice, have more complicated charging curves and strict charging and discharging rates, making them non-ideal for this application. However, supercapacitors have the disadvantage of having low capacity and linear charge vs voltage curves. When charging supercapacitors, balancing is crucial as each cell should not exceed its rated voltage, else the cell will be damaged. Simply applying a voltage to a set of capacitors might unevenly charge the supercapacitors, so a balancing circuit, Figure 12, was used, which had operational amplifier buffers to cut the applied voltage into fourths and apply the reduced voltage to each cell.

4.4.3 Motors

Motors convert electrical energy into mechanical energy. More specifically, current drawn by a motor induces a changing magnetomotive force (MMF). That changing MMF exerts a torque on the motor shaft, causing it to rotate. We used two low-power (6V), encoded (48 CPR encoder) cylindrical brushed DC gearmotors with a gear ratio of 9.7:1 from Polulo in a differential-drive arrangement (i.e. independently controlled motors).[4] To choose the optimal motor for this project, we calculated its efficiency, $\eta = P_{mech.}/P_{elec.}$, where $P_{mech.}$ and $P_{elec.}$ are the mechanical energy and electrical energy needed to drive the device, respectively (see the *Motor Dynamics* appendix section for more details).

4.4.4 Motor Controller

The motor controller controlled how much voltage and current was sent to the motor, dictating its speed and torque. To efficiently use the supercapacitor energy, we

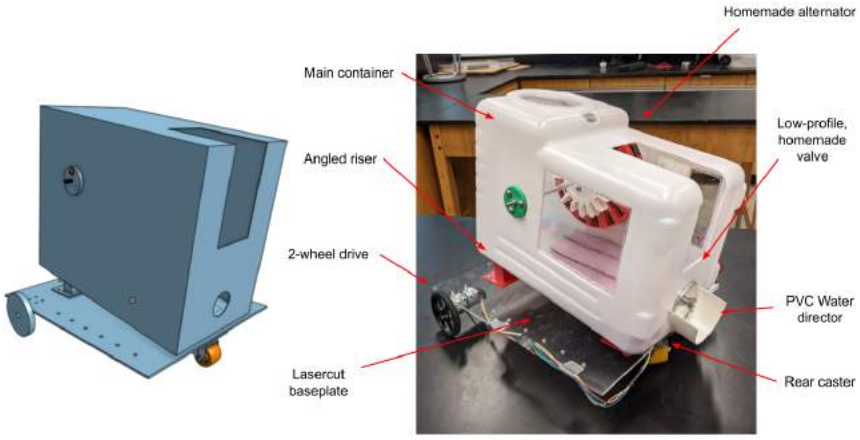

FIGURE 9: Isometric CAD and actual image (labeled) of the entire device.

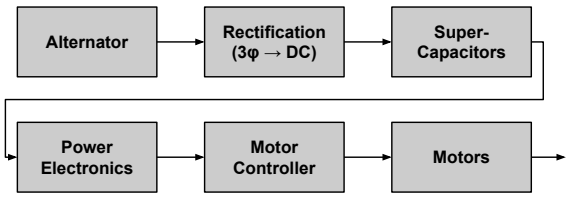

FIGURE 10: Block diagram of the electronics on the cart. *Note*: 3ϕ means 3-phase AC.

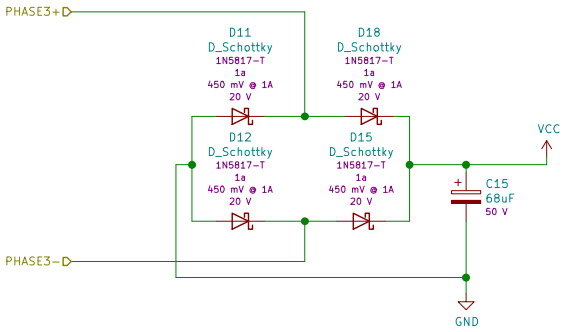

FIGURE 11: Full bridge diode rectifier used to turn the generated AC power into DC power.

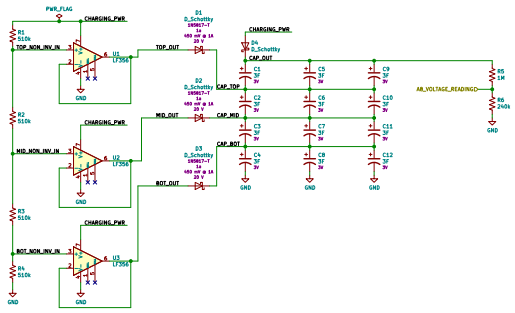

FIGURE 12: Circuit used to charge the supercapacitors.

planned on implementing a PID speed cascaded controller on the motors to set the device speed and orientation (see *Feedback Control*) based on the user through the Arduino bluetooth controller (see *Bluetooth Remote Controller*). To improve the power usage, multiple controllers were tested, including purchased and custom-made options (see *Motor Controller* for more details).

- **Arduino Motor Shield**: This controller was easy to interface with Arduino, but had a $1.2V$ drop from the capacitors to motors.
- **Purchased H-Bridge (BTS7960)**: This controller did not have a voltage drop, but had a minimum operating voltage, so the controller stopped working if the capacitors dropped below $\sim 4V$.
- **Custom-Made Mosfet H-Bridge**: This was a custom-made controller using Mosfets. It had a $1.5V$ drop from the capacitors to the motors.
- **Custom-Made Relay H-Bridge & Mosfet**: This was another custom-made design. It had a voltage drop of $0.6V$.
- **Custom-Made Relay H-Bridge**: This was also a custom-made H-bridge that only used relays. There was no voltage drop, but this was at the expense of speed control.

As can be seen in the motor controller circuit in Figure 13, DC voltage from the supercapacitors was used to power the motors. There were two relays in the circuit, where one relay was used to connect the capacitors to the motors and the second relay was used as an H-bridge with an NPN BJT (bipolar junction transistor) to control the motor speed via PWM. Using a custom relay H-bridge allows for the design to use every last bit of power in the supercapacitors to maximize the distance traveled. But, due to issues implementing the PID speed cascaded controller, the relay-only controller was used for the competition and no PID was used.

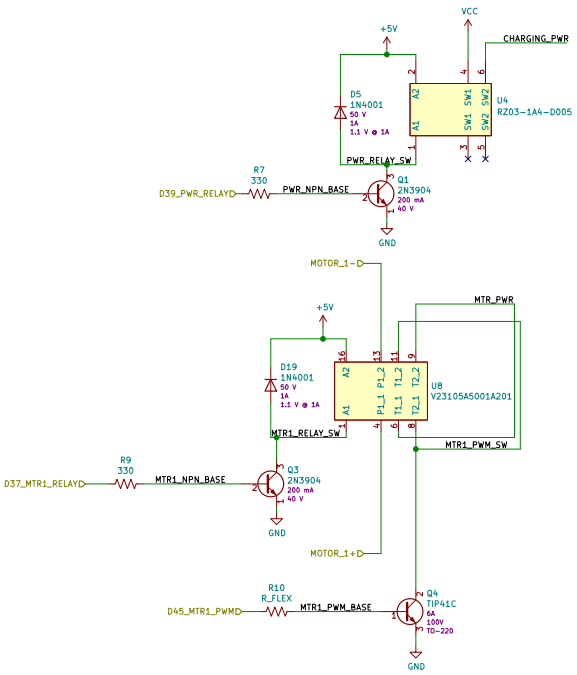

FIGURE 13: Circuit used to control the motors.

4.4.5 PCB

A Printed Circuit Board (PCB) was designed (see Figure 14) because PCBs are more consist/reliable than breadboards and a well-designed PCB keeps the connections organized. The PCB was designed as an expansion board to an Arduino MEGA, and included room for 12 supercapacitors, an LCD (liquid crystal display), the three rectifier circuits, and the relays for power and motor control. Four mounting holes were available to secure the PCB to the cart.

The PCB was not manufactured in in time to be used for competition.

4.5 Main Assembly

The device assembly, seen in Figure 9, had two main parts, the container with the alternator inside and the baseplate with the wheels and electronics. The container was mounted to two risers on the baseplate that held the container at an angle to allow it to drain. The baseplate was made of $4.5\,mm$ acrylic (see the *Baseplate FEA* for the structural analysis), which had laser-cut holes to mount the various components. The entire assembly weighed about $4.4\,kg$. In communicating with all the electronics, an Arduino Mega was used and mounted next to the water container. Code for the program can be found on Github. [5]

5 TESTING AND COMPETITION

5.1 Testing and Competition Setup

While testing various components, we had the device next to the sink, as illustrated in Figure 15a, so we could easily drain the water. A tube connected the faucet to the suspended bucket, giving the desired potential energy from its height. The nozzle, which was directed at the Pelton turbine, was connected to a tube that came down from the bucket.

For the final competition, the charging setup, Figure 15b, was improved in two main ways. (1) The device was moved to the ground, increasing the height difference to increase the pressure and flow rate. (2) A vortex reducer was added to the bucket to prevent air from being sucked down instead of water. These two changes resulted in a 48% reduction in charging time.

5.2 The Competition

The day of the competition was filled with a lot of troubleshooting and testing. It had been clear before then that the device had controllability issues, but none of the attempts to fix that issue were very successful. We made multiple attempts to record a successful run for submission, but each time the device would veer in an undesired direction and not reach the unloading zone. After spending nearly 15 hours that day trying to get the device to work properly, we decided to submit the best run we had recorded.

5.2.1 Controllability Issues

As mentioned, there were controllability issues with the device. Although we are unsure what exactly was the cause, there are some possible contributing factors (and the reason could be some, all, or something else).

1. **Bad motor**: While testing the motors off the ground, one motor seemed stronger than the other, possibly contributing to the veering.

2. **Unequal weight distribution**: The side-mounted alternator put the center of mass to the side, loading one wheel more than the other. Shifting the container to better center the mass caused the device drive straighter.

3. **Motor voltage threshold**: The motors had a minimum operating voltage. Once the capacitors dropped too low, the motors stopped running.

4. **No PID**: The relay controller could only be on or off, so there was no speed control for the motors. Thus, the device was running the motors at maximum voltage and could not adjust wheel velocities to correct its orientation.

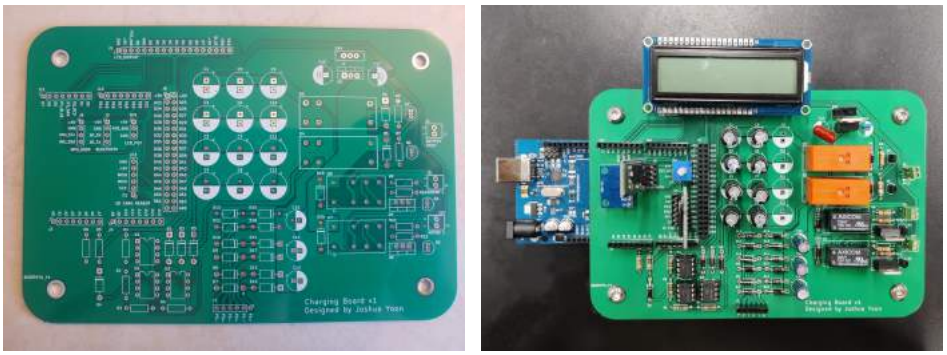

(a) PCB from the Manufacturer

(b) Assembled PCB

FIGURE 14: PCB designed to house the electronics for the design. (a) The PCB comes as an empty board that needs to be populated with parts. (b) The board parts were added and soldered by hand. The PCB can be seen attached to the Arduino (left side of the figure).

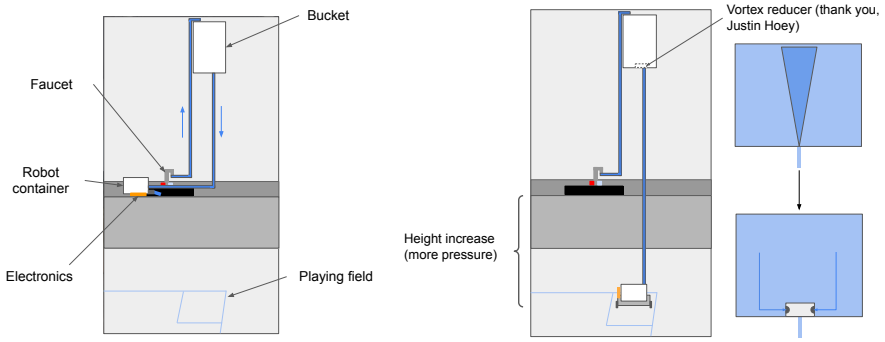

(a) Testing Setup

(b) Competition Setup

FIGURE 15: (a) Setup used to test the device (b) Setup used for the competition. Extra height and adding a vortex reducer reduced the charging time by 48%.

5. **No PCB**: The PCB was not ready for the competition, so breadboards were used. The wires and electronic components would sometimes fall out or short, interfering with the proper function.

5.2.2 Where Did the Energy Go?

After running many tests, it was apparent that the device was not harvesting and using nearly as much energy as it should have been. The Sanky diagram in Figure 16 shows the sources of energy and where the energy ended up. Despite the Pelton turbine operating at 74% of the peak efficiency, only a small amount of energy ended up being collected by the turbine (see the *Energy Loss Calculations* section). Pelton turbines operate best when the fluid has a high flow rate, but due to height limitations, the bucket couldn't be raised higher, which would have increased the flow rate and increase the amount of energy collected. Despite optimizing the stator coils, they were not manufactured exactly to the specification, reducing the alternator efficiency. Also, the rotor was not mounted as close as desired to the stator (because the coils were thicker than designed), which would have reduced the magnetic flux passing through the stator. Lastly, the motors were very inefficient and stopped working once the voltage reached about 2.5V, leaving unusable charge in the capacitors.

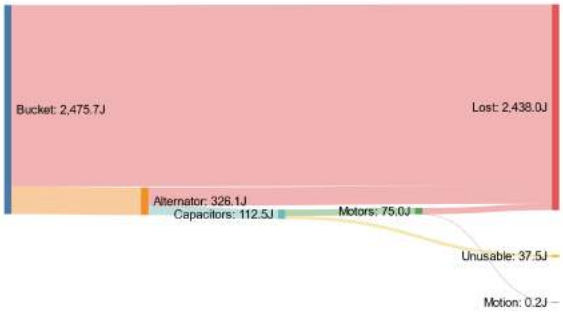

FIGURE 16: A Sanky diagram showing where the energy started (left) and where it went (right).

6 CONCLUSION

Throughout our senior year, we managed to design and build a small, upgradeable, water-powered, remote-controlled device for the 2022 ASME Student Design Competition. The device used a custom-made alternator, had a PCB for the electronics, and used a custom-made motor controller. Our design went through multiple design iterations where we were able to triple the driving distance and reduced charging time by 48%. In the end, we tied for 2nd best design (out of 17 teams).

6.1 Future Work

The controllability should be addressed first since that would make the device usable and more efficient. With the PCB now in possession, the device should be tested with the more reliable electronics. A possible efficiency improvement to the alternator would be to use metal plates on the outside of the rotor and stator to direct more of the magnetic field to the stator. This was attempted during testing, but was unsuccessful, possibly due to the wrong material being used. Lastly, the Pelton turbines were printed using an extrusion 3D printer, but future turbines should be printed using a resin printer for a better surface finish and stronger part.

ACKNOWLEDGEMENTS

Thank you to Sinisa Janjusevic, for his help with manufacturing some of the parts, Mike Giglia, for answering electronics questions and helping troubleshoot some problems, and Justin Hoey (ME'22), for helping us find the vortex-reducer design we used for our bucket.

REFERENCES

[1] ASME. 2021. URL: https://efests.asme.org/getattachment/Competitions/Student-Design-Competition-(SDC)/2022-SDC-Rules_FINAL.pdf.aspx?lang=en-US (visited on 09/03/2021).

[2] D S Benzon, G A Aggidis, and J S Anagnostopoulos. "Development of the Turgo Impulse Turbine: Past and Present". In: *Applied Energy* 166 (Dec. 2015), pp. 1–18. DOI: 10.1016/j.apenergy.2015.12.091.

[3] Eugene A. Avallone, Theodore Baumeister, and Robert D. Steele. *Marks Standard Handbook for Mechanical Engineers*. McGraw-Hill, 2006.

[4] Pololu. *Pololu - 9.7:1 metal gearmotor 25dx63l mm LP 6V with 48 CPR encoder*. 2022. URL: https://www.pololu.com/product/4822 (visited on 12/12/2021).

[5] Brandon Ho. *Arduino Code*. 2022. URL: https://github.com/BrandonGel/ME393-4/tree/main/Motor_Speed_Control7 (visited on 05/08/2022).

[6] McMaster. *McMaster, Low-Profile Swivel Caster with 1-3/8" Diameter Brown Polyurethane Wheel*. 2022. URL: https://www.mcmaster.com/4778T51/ (visited on 12/12/2021).

[7] Engineering Toolbox. *Engineering ToolBox, (2004). Friction - Friction Coefficients and Calculator*. 2022. URL: https://www.engineeringtoolbox.com/friction-coefficients-d_778.html (visited on 12/12/2021).

[8] Evonik Cyro LLC. *Acrylite cast GP physical properties*. 2022. URL: https://cdn.shopify.com/s/files/1/1408/9874/files/1235e-acrylite-cast-gp-physical-properties.pdf?4795133065712091057 (visited on 02/15/2022).

[9] Philip M. Gerhart, Andrew L. Gerhart, and John I. Hochstein. *Munson, Young, and Okiishi's Fundamentals of Fluid Mechanics*. Wiley, 2016.

7 APPENDIX

7.1 Mechanical Design

7.1.1 Mechanical Overview

Mechanical energy is classified into two forms, potential and kinetic. Potential energy is associated with a mass's position relative to some reference point, such as the water held some height above the device. Kinetic energy is energy associate with motion, and this is the energy the device needs to posses in order to move. So, the goal is to convert the potential energy of the water in the loading area to kinetic energy.

If the device were to immediately start using the kinetic energy that was being generated, then it would be difficult to load all the water in. Therefore, an energy storage system is needed. Unlike the electrical system that would use a battery or capacitor to store energy in the form of chemical or electrical potential energy, the mechanical energy can be stored as kinetic energy in a flywheel. A flywheel is a mechanical battery, storing kinetic energy through the conservation of angular momentum when it is spun.

For this project, a flywheel was theorized to have radial blades such that poured water could apply a torque, spinning the flywheel, as shown in Figure 17; this will be referred to as "charging" the flywheel.

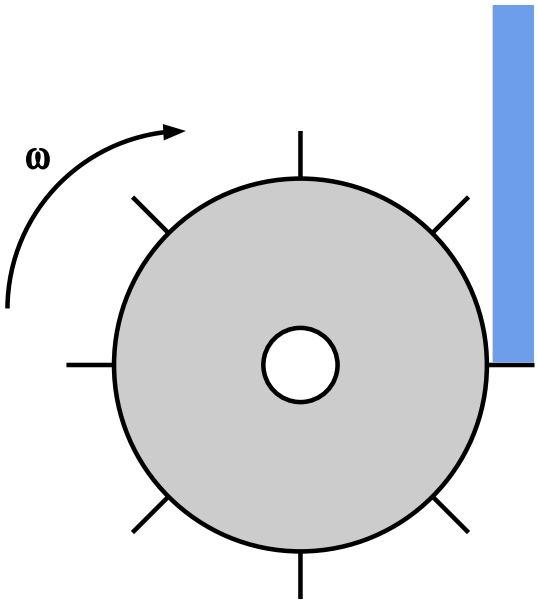

FIGURE 17: Water is poured against the blades of the flywheel, spinning it up, and "charging" the system as water is converted from potential energy to angular kinetic energy as storage.

The process used by the mechanical system, as outlined in Figure 18, requires few steps, reducing the avenues of energy loss over the entire system. The basic process involves the flywheel being spun, storing energy as angular kinetic energy. Once ready to use, the clutch would be engaged, transferring energy from the flywheel to the wheels on the ground, driving the cart.

FIGURE 18: Block diagram outlining the energy conversion process for the mechanical design option.

7.1.2 Energy

Angular kinetic energy, KE, of an object is a function of its moment of inertia, I, and angular velocity, ω as shown in Eq. (5).

$$KE = \frac{1}{2} I \omega^2 \tag{5}$$

This is the amount of energy possessed by the object. For this project, a flywheel will be used. When spun, it acts like a mechanical battery, storing energy as angular kinetic energy.

7.1.3 Moment of Inertia

The moment of inertia of the flywheel depends on the geometry of the flywheel, but for the sake of simplicity, a disk-shaped flywheel is considered. This is a baseline so that any improvements on the flywheel design will perform better than calculated. The moment of inertia of a disk with a hole in the center (for a shaft) when spun about its axis of symmetry is show in Eq. (6).

$$I_{fly} \approx I_{disk} = 0.5 \left(m_{solid} r_{outer}^2 - m_{hole} r_{hole}^2 \right) \tag{6}$$

m_{solid} is the mass of the disk if it did not have the hole and m_{hole} is the mass removed from the disk to make the shaft hole.

7.1.4 Angular Velocity

The angular kinetic energy of the flywheel depends on the applied force from the water. This can be calculated using the conservation of momentum for fluids shown in Eq. (7).

$$\sum F_{ext,y} = \frac{\partial}{\partial t} \int_{CV} \rho V_y \, \mathrm{d}V + \int_{CS} \rho V_y \left(\vec{V} \cdot \hat{n} \right) \, \mathrm{d}A \tag{7}$$

where ρ is the water density, V_y is the y-component of the fluid velocity, and $\hat{n}$ is the normal vector to the control surface. The specific situation being modeled is shown in Figure 19. For simplicity, only a flat turbine blade is considered. Not shown is the flywheel, which would be to the right of the turbine blade. This can be ignored because only small time steps are being analyzed, during which the turbine blade would be moving nearly linearly (vertically).

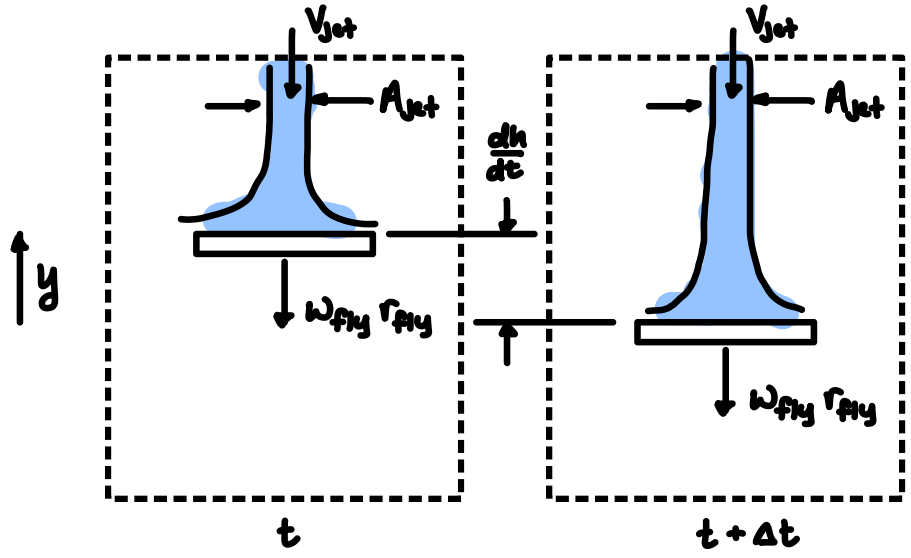

FIGURE 19: Control volume and fluid before and after a small time step Δt for conservation of fluid momentum.

The LHS of Eq. (7) is the applied, downward force of the water, F_w. The from the first term on the RHS, the density and velocity can be pulled out, since the fluid is assumed to be incompressible, not accelerating (at least

not significantly), and not a function of volume.

$$\frac{\partial}{\partial t}\int_{CV}\rho V_y\,\mathrm{d}V \approx \rho V_y\frac{\partial}{\partial t}\int_{CV}\mathrm{d}V \tag{8}$$

The integrated volume is just the volume, and taking the derivative of that volume is the change in volume between time t and time $t+\Delta t$.

$$\frac{\partial}{\partial t}\int_{CV}\mathrm{d}V = \frac{\partial}{\partial t}(V) = A_{jet}\frac{\mathrm{d}h}{\mathrm{d}t} = \omega_{fly}r_{fly}A_{jet} \tag{9}$$

The second term on the RHS accounts for the flow passing through the control surface in the y-direction. Since it only enters at the top (going in the opposite direction of the outward-pointing surface normal), and exits laterally, only the top portion needs to be considered. Again, the density and velocity are constant with respect to area, so they can be pulled out of the integral, only leaving the integral of the area which equals the area. The second term from the RHS is then found to be

$$-\rho V_{jet}^2 A_{jet} \tag{10}$$

Combining all the terms and solving for the force of the water yields

$$F_w = \rho V_{jet}A_{jet}(V_{jet} - \omega_{fly}r_{fly}) \tag{11}$$

The time-varying angular velocity of the flywheel can be found by using Newton's second law for rotation shown in Eq. (12).

$$\sum\tau = I\alpha \tag{12}$$

where τ is the applied torque and α is the angular acceleration, which is the first derivative of angular velocity, i.e. $\alpha = \dot{\omega}$. Applying the water force at a moment arm of r_{fly} yields the following differential equation

$$\rho V_{jet}A_{jet}(V_{jet} - \omega_{fly}r_{fly})r_{fly} = I_{fly}\dot{\omega}_{fly} \rightarrow \dot{\omega_{fly}} + \frac{\rho V_{jet}A_{jet}r_{fly}^2}{I_{fly}}\omega_{fly} = \frac{\rho V_{jet}^2 A_{jet}r_{fly}}{I_{fly}} \tag{13}$$

The flywheel initially starts at rest, i.e. $\omega_{fly}(0) = 0$. The homogenous solution can be solved using an exponential trial solution.

$$\omega_{fly,h}(t) = Ce^{\lambda t} \rightarrow \frac{\mathrm{d}}{\mathrm{d}t} \rightarrow \dot{\omega}_{fly,h}(t) = C\lambda e^{\lambda t} \tag{14}$$

$$\cancel{C\lambda e^{\lambda t}} + \cancel{Ce^{\lambda t}}\frac{\rho V_{jet}A_{jet}r_{fly}^2}{I_{fly}} = 0 \rightarrow \lambda = -\frac{\rho V_{jet}A_{jet}r_{fly}^2}{I_{fly}} \tag{15}$$

$$\Rightarrow \omega_{fly,h}(t) = Ce^{-\frac{\rho V_{jet}A_{jet}r_{fly}^2}{I_{fly}}t} \tag{16}$$

The particular solution can be found by looking at the form of the differential equation and noting that the RHS is a constant, so $\omega_{fly,p}(t)$ must also be a constant. Plugging in $\omega_{fly,p}(t) = k\text{constant}$ yields

$$0 + k\frac{\rho V_{jet}A_{jet}r_{fly}^2}{I_{fly}} = \frac{\rho V_{jet}^2 A_{jet}r_{fly}}{I_{fly}} \Rightarrow \omega_{fly,p}(t) = k = \frac{V_{jet}}{r_{fly}} \tag{17}$$

Combining the homogeneous and particular solutions yields

$$\omega_{fly}(t) = Ce^{-\frac{\rho V_{jet}A_{jet}r_{fly}^2}{I_{fly}}t} + \frac{V_{jet}}{r_{fly}} \tag{18}$$

Applying the initial condition

$$\omega_{fly}(0) = 0 = C(1) + \frac{V_{jet}}{r_{fly}} \rightarrow C = -\frac{V_{jet}}{r_{fly}} \tag{19}$$

Therefore, the final equation for the flywheel angular velocity versus time is

$$\boxed{\omega_{fly}(t) = \frac{V_{jet}}{r_{fly}}\left(1 - e^{-\frac{\rho V_{jet}A_{jet}r_{fly}^2}{I_{fly}}t}\right)} \tag{20}$$

7.1.5 Clutch Energy Transfer

Once the flywheel is charged up, the energy from the flywheel needs to be transferred to the wheels of the cart in order to move it. This will be achieved through the use of a clutch. Once engaged, the clutch, which will be chained to the driveshaft, transferring energy from the flywheel to the wheels on the ground. Before the clutch is engaged (Figure 20a), the angular velocity of the flywheel will be the final angular velocity from charging, and the angular velocity of the cart's wheels will be zero, since the cart will be stationary. After engaging the clutch (Figure 20b), the angular velocity of the flywheel and cart wheels will be coupled through their gearing ratio, as shown in Eq. (21).

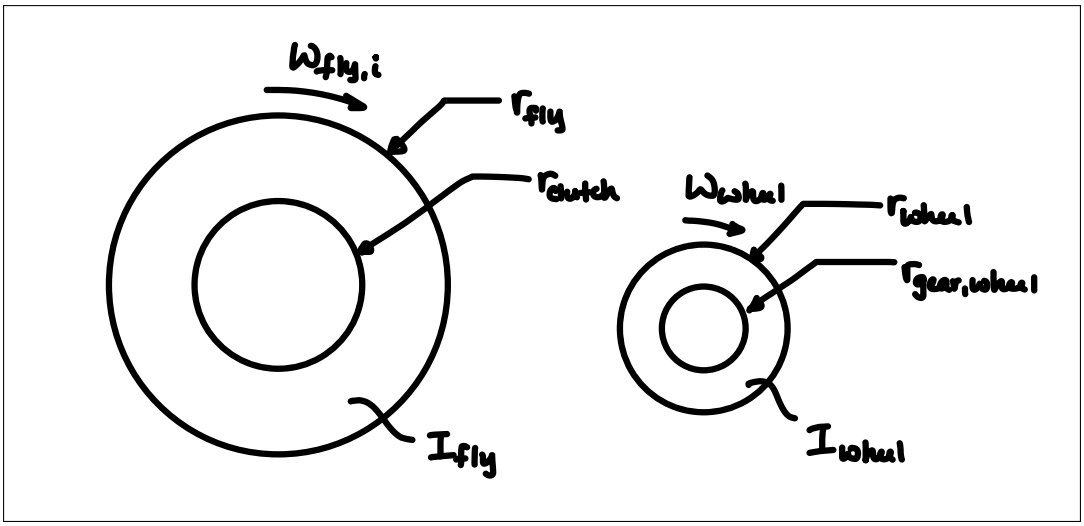

(a) Before

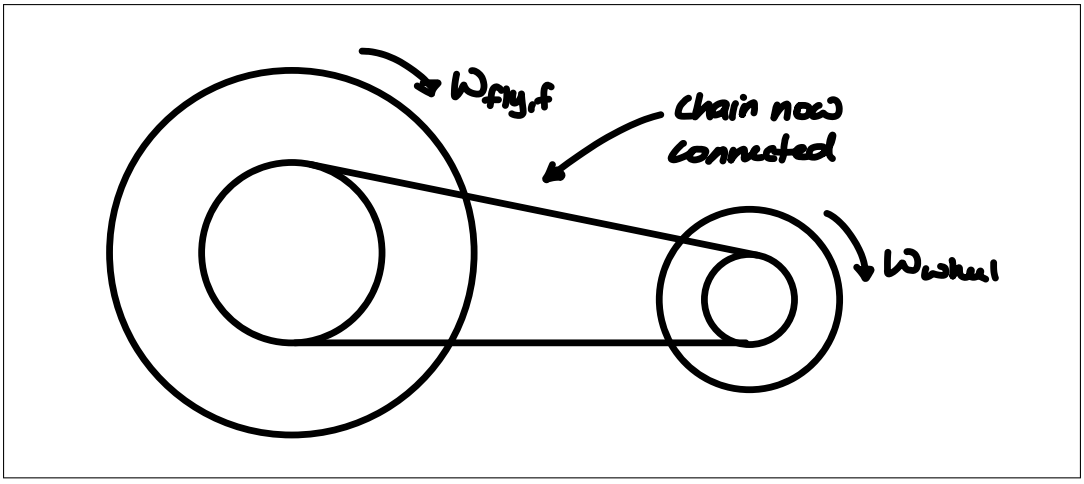

(b) After

FIGURE 20: Flywheel and cart wheel system (a) before and (b) after engaging the clutch.

$$\omega_{fly,f} r_{clutch} = \omega_{wheel} r_{gear,wheel} \tag{21}$$

where $\omega_{fly,f}$ is the angular velocity of the flywheel after engaging the clutch, r_{clutch} is the radius of the clutch, ω_{wheel} is the wheel angular velocity after engaging the clutch, and $r_{gear,wheel}$ is the radius of the radius of the driven component of the wheel connected to the clutch via the chain. To calculate the calculate the angular velocity of the wheels after engaging the the clutch, the law of conservation of angular momentum will be used for both the flywheel and the cart wheels and the conservation of linear momentum for the entire cart. This can be determined through an analysis of the free body diagram shown in Figure 21, resulting in the equation shown in Eqs. (22), (23), (24).

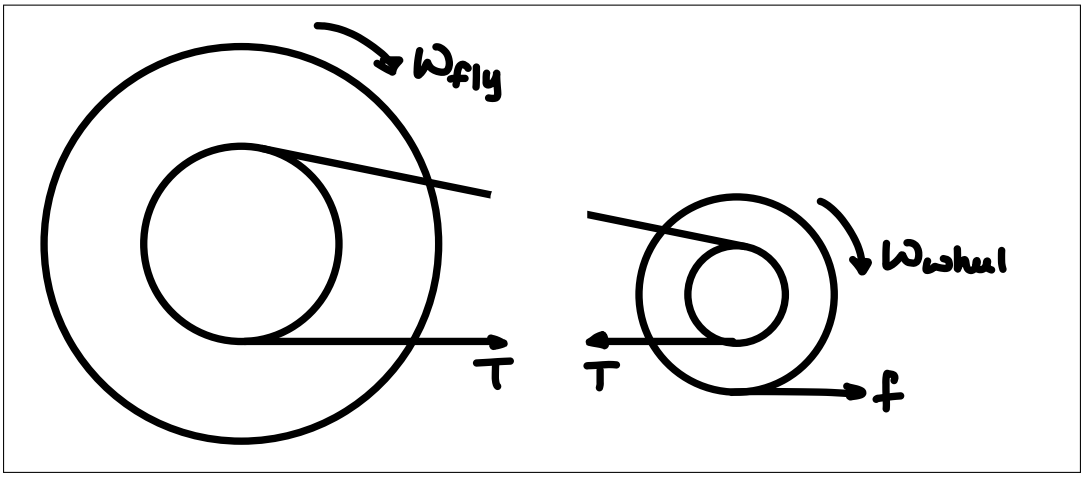

FIGURE 21: Free body diagram of the mechanical system, specifically of the flywheel and cart wheels connected via a chain.

$$I_{fly}(\omega_{fly,f} - \omega_{fly,i}) = Tr_{clutch}\Delta t \tag{22}$$

$$2I_{wheel}(\omega_{wheel} - 0) = fr_{wheel}\Delta t - Tr_{gear,wheel}\Delta t \tag{23}$$

$$m_{cart}(v_{cart} - 0) = f\Delta t \qquad \text{where no slip means: } v_{cart} = -r_{wheel}\omega_{wheel} \tag{24}$$

where $\omega_{fly,i}$ and $\omega_{fly,f}$ are the initial and final flywheel angular velocities, corresponding to before and after engaging the clutch, T is the chain tension, Δt is some small time interval over which the conservation law is applied, f is the friction from the ground, and v_{cart} is the linear velocity of the cart after engaging the clutch. The moment of inertia is doubled in Eq. (23) because there are two driven wheels. Solving Eqs. (22) and (23) for $T\Delta t$ allows the two resulting equations to be equated.

$$\left.\begin{aligned} T\Delta t &= \frac{I_{fly}(\omega_{fly,f} - \omega_{fly,i})}{r_{clutch}} \\ T\Delta t &= \frac{fr_{wheel} - 2I_{wheel}\omega_{wheel}}{r_{gear,wheel}} \end{aligned}\right\} \frac{I_{fly}(\omega_{fly,f} - \omega_{fly,i})}{r_{clutch}} = \frac{fr_{wheel} - 2I_{wheel}\omega_{wheel}}{r_{gear,wheel}} \tag{25}$$

Eq. (24) can be rearranged for $f\Delta t$ and then plugged into Eq. (25), yielding

$$\frac{I_{fly}(\omega_{fly,f} - \omega_{fly,i})}{r_{clutch}} = -\frac{m_{cart}r_{wheel}^2 + 2I_{wheel}}{r_{gear,wheel}}\omega_{wheel} \tag{26}$$

To remove dependence on the final flywheel angular velocity, Eq. (21) can be plugged into Eq. (26) and then solved for the wheel angular velocity, which is the desired result.

$$\boxed{\omega_{wheel} = \frac{I_{fly}}{\frac{r_{gear,wheel}}{r_{clutch}}I_{fly} + 2\frac{r_{clutch}}{r_{gear,wheel}}I_{wheel} + \frac{r_{clutch}r_{wheel}^2}{r_{gear,wheel}}m_{cart}}\omega_{fly,i}} \tag{27}$$

7.2 Stator Optimization

The variables that were optimized were the inner and outer radii of the 6 stator coils as well as the number of magnet wire turns for each coil. Limitations on the variables were set to ensure the design could be manufactured, such as a limitation on the maximum coil radius and a maximum number of wire turns per coil. The optimization was performed in Python using the GEKKO dynamic optimization package with the goal of maximizing the power produced by each coil. The optimal coil design had an inner radius of $0.0254\,m$, outer radius of $0.0762\,m$, and optimal number of wire turns of 945, which should produce $1.527\,W$.

Below is the Python code used for the optimization. The GEKKO package makes it very simple to setup and solve an optimization problem, with different class methods for adding decision variables variables (`Var`), derived parameters as functions of decision variables (`Intermediate`), constraints (`Equation`), and the objective function

$$
\begin{aligned}
\text{maximize} \quad & \frac{V^2}{\Omega_{coil}} && \text{(28a)}\\
\text{subject to} \quad & t_{coil} = \frac{N_{turns}\pi\left(\frac{d_{wire}}{2}\right)^2}{0.91\, d_{coil}} && \text{(28b)}\\
& \bar{A}_{coil} = \frac{\theta_{coil}}{2\pi}\pi\left[\left(r_{outer} - \frac{t_{coil}}{2}\right)^2 - \left(r_{inner} + \frac{t_{coil}}{2}\right)^2\right] \\
& \qquad - 2\left(\frac{t_{web}}{2} + \frac{t_{coil}}{2}\right)\left[\left(r_{outer} - \frac{t_{coil}}{2}\right) - \left(r_{inner} + \frac{t_{coil}}{2}\right)\right] && \text{(28c)}\\
& \frac{\mathrm{d}B}{\mathrm{d}t} = \frac{2B_{mag}}{\theta_{mag.}/\omega_{rotor}} && \text{(28d)}\\
& V = -N_{turns}\frac{\mathrm{d}B}{\mathrm{d}t}A_{coil} && \text{(28e)}\\
& \ell_{turn} = \theta_{coil}(r_{outer} + r_{inner}) + 2\left[\left(r_{outer} - \frac{t_{coil}}{2}\right) - \left(r_{inner} + \frac{t_{coil}}{2}\right)\right] && \text{(28f)}\\
& \Omega_{coil} = \ell_{turn}N_{turns}\Omega_{wire} && \text{(28g)}\\
& r_{inner,min} \le r_{inner} \le r_{inner,max} && \text{(28h)}\\
& r_{outer,min} \le r_{outer} \le r_{outer,max} && \text{(28i)}\\
& 1 \le N_{turns} \le -45059.7\, r_{inner} + 144107.3\, r_{outer} && \text{(28j)}\\
& t_{coil} \le t_{coil,max} && \text{(28k)}\\
& r_{inner},\, r_{outer},\, t_{coil},\, \bar{A}_{coil},\, \mathrm{d}B/\mathrm{d}t,\, V,\, \ell_{turn},\, \Omega_{coil} \in \mathbb{R}\\
& N_{turns} \in \mathbb{Z}
\end{aligned}
$$

Where:
$\omega_{rotor} = 14.2\, rad/s$
$B_{mag} = 0.142\, T$
$N_{coils} = 6$
$\theta_{coil} = 0.785\, rad$
$N_{mag} = 8$
$\theta_{mag.} = 1.047\, rad$
$t_{web} = 0.005\, m$
$d_{coil} = 0.01\, m$
$t_{coil,max} = 0.01\, m$
$r_{outer,min} = 0.0454\, m$
$r_{outer,max} = 0.0762\, m$
$r_{inner,min} = 0.0254\, m$
$r_{inner,min} = 0.0354\, m$
$d_{wire} = 0.00035\, m$
$\Omega_{wire} = 0.211\, ohm/m$

Equation 28: The "full" Lagrange formulation of the optimization problem.

to be, in this case, maximized (`Maximize`). The problem was not simplified, since the package can handle the simplification without any issue.

```
# -*- coding: utf-8 -*-
"""
Jared Jacobowitz
Spring 2022
CHE488 Convex Optimization Techniques
Stator Coils Optimization

This code optimizes the stator coil design to maximize power
"""
from gekko import Gekko
import numpy as np

# ================================================================================
# Parameters
# ================================================================================
w_rotor = 14.2          # [rad/s]; angular velocity of the rotor (measured)
B = 0.142               # [T]; magnetic field strength (measured)
N_mag = 8               # [-]; number of magnets on the rotor
N_coils = 6             # [-]; number of coils on the stator
t_web = 0.005           # [m]; web thickness between each stator coil
depth_coil = 0.01       # [m]; depth of the coils into the stator
t_coil_max = 0.01       # [m]; maximum thickness of the stator coils
r_outer_min = 0.0454    # [m]; minimum outer radius of the coils
r_outer_max = 0.0762    # [m]; maximum outer radius of the coils
r_inner_min = 0.0254    # [m]; minimum inner radius of the coils
r_inner_max = 0.0354    # [m]; minimum inner radius of the coils
d_wire = 3.5e-4         # [m]; diameter of the magnet wire
ohm_wire = 0.211        # [ohm/m]; linear resistance of the wire (measured)

# ================================================================================
# Derived Parameters
# ================================================================================
theta_mag = 2*np.pi/N_mag       # [rad]; angle between magnets
dBdt = 2*B/(theta_mag/w_rotor)  # [T/s]; time-varying B-field
theta_coil = 2*np.pi/N_coils    # [rad]; angle of each coil

# ================================================================================
# Setting up the optimization problem
# ================================================================================
# Creating the model object
m = Gekko()

# Adding the decision variables
# [m]; stator coil outer radius
r_outer = m.Var(value=r_outer_min,
                lb=r_outer_min, ub=r_outer_max,
                name="r_outer")
# [m]; stator coil inner radius
r_inner = m.Var(value=r_inner_min,
                lb=r_inner_min, ub=r_inner_max,
                name="r_inner")
# [-]; turns per stator coil
N_turns = m.Var(value=1,
                lb=1,
                name="N_turns", integer=True)


# Derived values
# (turns)*(wire area)/(circle packing)/(coil depth)
# [m]; coil thickness
t_coil = m.Intermediate(N_turns*np.pi*(d_wire/2)**2/0.91/depth_coil)

# [m^2]; coil area
A_coil = m.Intermediate(np.pi*((r_outer - t_coil/2)**2
                               - (r_inner + t_coil/2)**2) * theta_coil/2/np.pi
                        - t_web*((r_outer - t_coil/2) - (r_inner + t_coil/2))
                        )
```

```
68
69  # [V]; emf from Faraday's Law
70  V = m.Intermediate(-N_turns*dBdt*A_coil)
71
72  # [m]; midline length of a coil turn
73  el_turn = m.Intermediate(2*((r_outer - t_coil/2)
74                              - (r_inner + t_coil/2))
75                           + theta_coil*(r_outer + r_inner)
76                           )
77
78  # [ohm]; resistance of a stator coil
79  ohm_coil = m.Intermediate(el_turn*N_turns*ohm_wire)
80
81
82  # [-]; discontinuity turns
83  N_discontinuity = m.Intermediate(-45059.7*r_inner
84                                   + 144107.3*r_outer
85                                   )
86
87  # Adding constraints
88  m.Equation(N_turns <= N_discontinuity)
89  m.Equation(t_coil <= t_coil_max)
90
91  # Defining the objective function
92  m.Maximize(V**2/ohm_coil)
93
94  # ================================================================================
95  # Solving
96  # ================================================================================
97  # IPOPT
98  m.options.SOLVER = 3
99  m.solve()               # turn off prints with disp=False
100
101 print()
102 print("Results")
103 print(f"{r_outer[0]=}")
104 print(f"{r_inner[0]=}")
105 print(f"{N_turns[0]=}")
106 print()
107
108
109 # APOPT
110 m.options.SOLVER = 1
111 m.solve()
112
113 print()
114 print("Results")
115 print(f"{r_outer[0]=}")
116 print(f"{r_inner[0]=}")
117 print(f"{N_turns[0]=}")
```

7.3 Motor Dynamics

Motor calculations were preformed in choosing the most efficient and suitable motors for driving our device under the given loading conditions. The first step is to find the torque needed to drive our device. The second step is to find the efficiency of the suitable motors. Several assumptions were made in characterizing the device and motors dynamics:

- The device is a rigid body.
- The weight of the device is uniform distributed.
- Ignore bearing friction, rolling friction, and air resistance.
- No slippage between the wheels and floor.
- Neglect inductance in the motors.
- Linear relationship among the motor torque, speed, and input current

Figure 22 displays the free-body diagram (FBD) of the device. The motors control the two big front wheels. The wheel caster is the small back wheel.

For driving the wheels, there is a moment T exerted by the motors which is counteracted by friction exerted by

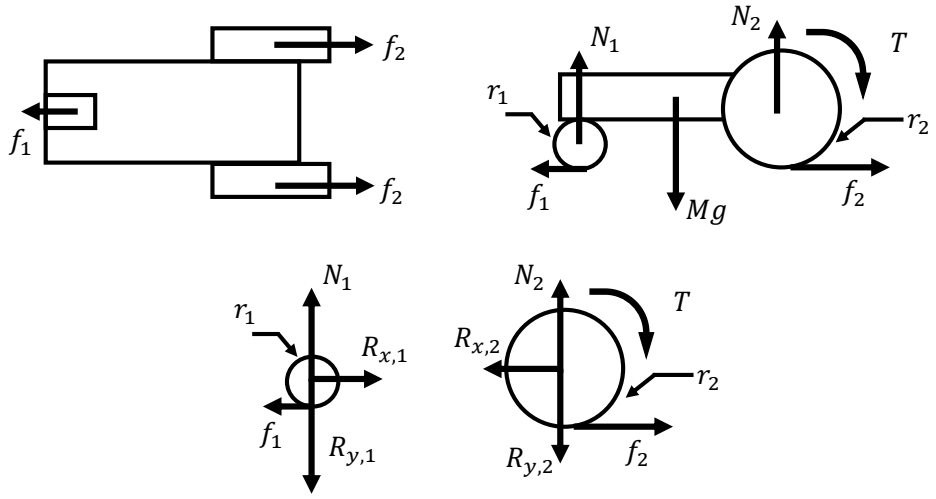

FIGURE 22: The top left FBD is for the top-view of the device. The top right FBD is for the side-view of the device. The bottom FBDs are for the wheels.

the floor f_2 at a distance of r_2 which is the front wheel radius. Friction from the floor is what accelerating the device. At the same, there is friction exerted by the floor f_1 onto the wheel caster at a distance of r_1 which is the wheel caster radius. Since gravity g exists, there is a gravitational force of Mg applied on the device where M is the mass of the device. Since the device is on the ground, there are also normal force N_1 and N_2 applied on the wheel caster and the big wheel, respectively. For the wheel caster and the front wheels FBD, there is a reaction forces exerted on each wheel: $R_{x,1}$ which pulls the wheel caster forward, $R_{x,2}$ which pulls on the front wheels backward, $R_{y,1}$ which pushes the wheel caster down, $R_{y,2}$ which pushes on the front wheels down.

The forces and moments on the device and wheel can be calculated by Newton's Second Law of Motion.

$$\sum F_{net,x} = Ma_x \tag{29}$$

$$\sum F_{net,y} = Ma_y \tag{30}$$

$$\sum T_{net} = I_\alpha \tag{31}$$

$$\sum T_{net,1} = I_1\alpha_1 \tag{32}$$

$$\sum T_{net,2} = I_2\alpha_2 \tag{33}$$

a_x and a_y are the acceleration of the device horizontally and vertically, respectively. α α_1 and α_2 are the angular acceleration of the device with respect to the wheel caster, wheel caster, and front wheel, respectively. I_1 and I_2 are the moment of inertia of the the wheel caster and front wheel, respectively.

Here are the system of equations.

$$Ma_x = 2f_2 - f_1 \tag{34}$$
$$Ma_y = N_1 + 2N_2 - Mg \tag{35}$$
$$I_\alpha = N_2 l - \frac{Mgl}{2} \tag{36}$$
$$I_1\alpha_1 = -f_1 r_1 \tag{37}$$
$$I_2\alpha_2 = f_2 r_2 - T \tag{38}$$
$$\alpha = 0 \tag{39}$$
$$a_x = -\alpha_1 r_1 \tag{40}$$
$$a_x = -\alpha_2 r_2 \tag{41}$$
$$a_y = 0 \tag{42}$$
$$0 = N_1 - R_{y,1} \tag{43}$$
$$0 = N_2 - R_{y,2} \tag{44}$$
$$f_1 \leq \mu_{s,1} N_1 \tag{45}$$
$$f_2 \leq \mu_{s,2} N_2 \tag{46}$$
$$\tag{47}$$

l is the length of the device. Since the device weight is uniform, the moment arm due to gravity is $\frac{l}{2}$ $a_y = 0$ and $\alpha = 0$ since the device is not falling and not rotating around the wheel caster. Since there is no slippage between the wheels and the ground, a_x is proportional to the α_1 and α_2 $\mu_{s,1}$ and $\mu_{s,2}$ are the static friction for wheel caster and the front wheel, respectively. f_1 and f_2 are bounded above the maximum static friction defined by $\mu_{s,1}N_1$ and $\mu_{s,1}N_1$ respectively.

Here are the solutions to the system of equation.

$$f_1 = \frac{I_1 a_x}{r_1^2} \tag{48}$$
$$f_2 = -\frac{I_2 a_x}{r_2^2} + \frac{T}{r_2} \tag{49}$$
$$N_1 = \frac{Mg}{2} \tag{50}$$
$$N_2 = \frac{Mg}{4} \tag{51}$$
$$T = \left(M + \frac{I_1}{r_1^2} + 2\frac{I_2}{r_2^2}\right) a_x \left(\frac{r_2}{2}\right) \tag{52}$$

The moment inertia terms in the moment equation can be neglect if it is small compared to the mass of the device. The device mass without water was calculated to be $3kg$ The average load for driving the device was assumed to be $2L$ of water. The wheel caster moment of inertia and radius were $3.11 \times 10^{-5} kg - m^2$ and $0.0174625m$[6] The front wheel moment of inertia and radius were $5.06 \times 10^{-5} kg - m^2$ and $0.4m$[4]

$$M = M_{no,water} + \rho_{water} V = 2kg + (997\frac{kg}{m^3})(2L)(10^-6\frac{m^3}{L}) = 4.994kg \tag{53}$$
$$\frac{I_1}{r_1^2} = \frac{3.11 \times 10^{-5}}{0.0174625m^2} = 0.102kg \tag{54}$$
$$\frac{I_2}{r_2^2} = \frac{5.06 \times 10^{-5}}{0.4m^2} = 0.0317kg \tag{55}$$
$$\frac{\frac{I_1}{r_1^2} + \frac{I_2}{r_2^2}}{M} = \frac{0.102kg + 0.0317kg}{4.994kg} \times 100\% = 2.68\% \tag{56}$$

Since ratio between the moment of inertia of the wheels and the device mass is about 2.68% which is less than 5%, the moment of inertia in the wheels in negligible in calculating the moment equation. The moment equation can be simplified in the following.

$$T = \frac{Ma_x r_2}{2} \tag{57}$$

The minimum torque to drive the device is proportional to the device acceleration. To minimize the torque input, there will be ramp input for the device to drive from rest to our desired speed. Our goal is to reach from the loading zone to the unloading zone ($3.356m$) in about 20 seconds. The average speed or desired speed v_{avg} of the device can be calculated.

$$v_{avg} = \frac{\Delta x}{\Delta t} = \frac{3.356m}{30s} = 0.177\frac{m}{s} \tag{58}$$

For finding the starting acceleration of the device, we chose 1 second for the acceleration time. Since there will be a ramp input for the device, its starting acceleration can be found.

$$a_x = \frac{\Delta v}{\Delta t} = \frac{0.177\frac{m}{s}}{1s} = 0.177\frac{m}{s^2} \tag{59}$$

Static friction coefficient was calculated to be 0.6[7]. Angular accelerations, forces, and moments on the devices can be calculated.

$$M = M_{no,water} + \rho_{water}V = 2kg + \left(997\frac{kg}{m^3}\right)(2L)\left(10^{-6}\frac{m^3}{L}\right) = 4.97kg \tag{60}$$

$$\alpha_2 = -\frac{a_x}{r_2} = -\frac{0.177\frac{m}{s^2}}{0.4m} = -4.419\frac{rad}{s} \tag{61}$$

$$f_1 = \frac{I_1 a_x}{r_1^2} = 0.018N \tag{62}$$

$$f_2 = \frac{I_2 a_x}{r_2^2} + \frac{T}{r_2} = 0.447N \tag{63}$$

$$N_1 = \frac{Mg}{2} = \frac{(4.97kg)\left(9.81\frac{m}{s^2}\right)}{2} = 24.496N \tag{64}$$

$$N_2 = \frac{Mg}{4} = \frac{(4.97kg)\left(9.81\frac{m}{s^2}\right)}{4} = 12.249N \tag{65}$$

$$f_{1,max} = \mu_s N_1 = (0.6)(24.496N) = 14.697N \tag{66}$$

$$f_{2,max} = \mu_s N_2 = (0.6)(12.249N) = 7.349N \tag{67}$$

$$T = \frac{Ma_x r_2}{2} = 0.0177Nm \tag{68}$$

The efficiency of the motor system η_{mech} is 40.13%. The power require to drive the motor P_{mech} is given by the following equation.

$$\omega_2 = \frac{v_{avg}}{r_2} = \frac{0.177\frac{m}{s}}{0.4m} = 4.419\frac{rad}{s} \tag{69}$$

$$P_{mech} = \frac{T\omega_2}{\eta_{mech}} = \frac{(0.0177Nm)\left(4.419\frac{rad}{s}\right)}{0.4013} = 0.36W \tag{70}$$

ω_2 is the angular velocity of the motors.

We chose one of the 9.7:1 25D Motor (Low Power) on Pololu for convenience and having familiarity in using their motors.[4] The motors on Pololu has the following characteristics: voltage rating V, no load speed $\omega_{no,load}$, no load current $I_{no,load}$, and stall current I_{stall}, stall torque T_{noload}. Some necessary derived parameters are calculated to define the motor.

$$R = \frac{V}{I_{stall}} = \frac{6V}{2A} = 3\Omega \tag{71}$$

$$k_\omega = \frac{\omega_{no,load}}{T_{noload}} = \frac{630rpm}{1.3kg-cm} = 484.62\frac{rpm}{kg-cm} \tag{72}$$

$$k_i = \frac{T_{no,load}}{I_{stall} - I_{noload}} = \frac{1.3kg}{2A - 0.12A} = 0.69\frac{kg-cm}{A} \tag{73}$$

$$k_b = \frac{V - I_{noload}R}{\omega_{no,load}} = \frac{6V - (2A)(3\Omega)}{630rpm} = 0.0090\frac{V}{rpm} \tag{74}$$

R is the resistance in the winding. k_ω is the torque-speed constant. k_i is the torque-current constant. k_b is the back EMF constant. The suitable motor must have a no load speed greater than our desired speed and a stall torque greater than our minimum required torque to drive the device. Next is to find the back EMF $\mathcal{E}$ current draw I_{draw} and voltage draw V_{draw} for the motors to drive the device.

$$\mathcal{E} = k_b\omega_2 = \left(0.0090\frac{V}{rpm}\right)\left(4.419\frac{rad}{s}\right)\left(\frac{60rev/s}{2\pi rad}\right) = 0.378V \tag{75}$$

$$I_{draw} = \frac{T}{k_i} + I_{noload} = \frac{(0.0177Nm)\frac{100cm/m}{9.81N/kg}}{0.69\frac{kg-cm}{A}} + 0.12 = 0.380A \tag{76}$$

$$V_{draw} = I_{draw}R + \mathcal{E} = (0.380A)(3\Omega) + 0.378V = 1.545V \tag{77}$$

The efficiency of the motor η can be calculated.

$$P_{loss} = I_{draw}R^2 = (0.380A)(3\Omega)^2 = 0.434W \tag{78}$$

$$P_{elec} = I_{draw}V_{draw} = (0.380A)(1.545V) = 0.574W \tag{79}$$

$$P_{in} = P_{elec} + P_{loss} = 1.008W \tag{80}$$

$$P_{out} = P_{mech} = 0.078W \tag{81}$$

$$\eta = \frac{P_{out}}{P_{in}} = \frac{0.078W}{1.008W} = 7.72\% \tag{82}$$

Even though efficiency of the motor is low, the crucial aspect is how much energy does the motor need to draw to drive the device from the loading zone to the unloading zone. Total input energy E_{in} needed to drive the device can be calculated.

$$V_{drive} = I_{noload}R + \mathcal{E} = (0.120A)(3\Omega) + 0.378V = 0.738V \tag{83}$$

$$P_{drive} = I_{noload}V_{drive} + I_{noload}R^2 = (0.12A)(0.738V) + (0.12A)(3\Omega)^2 = 0.132W \tag{84}$$

$$E_{in} = Pint_{accel} + P_{drive}t_{drive} = (1.008W)(1s) + (0.132W)(20s) = 3.689J \tag{85}$$

V_{drive} and P_{drive} is the voltage and power to drive the motor at desired speed, respectively. t_{accel} and t_{drive} is the time to accelerate device and drive the device at the desired speed, respectively. Thus, out of the motors we found in Pololu, we picked 9.7:1 25D Motor (Low Power).[4]

7.4 Motor Controller Iterations

In choosing the optimal motor controller for competition, we tested five different motor controllers, buying off-the-shelves ones and producing our own.

Figure 23 shows the first motor controller to be used for the device. The first motor controller was an off-the-shelve Arduino Motor Shield Rev3, which was easy to interface with Arduino, but had a 1.2V drop from the capacitors to motors due to its inefficient L298P chip.

FIGURE 23: Arduino Motor Shield Rev3

Figure 24 shows the second motor controller to be used for the device. The second one was an off-the-shelve external motor controller called BTS7960 which does not have a voltage drop from capacitors to motors, but had a minimum operating voltage to run. So, once the capacitors dropped too low (about 4V), the controller wouldn't work.

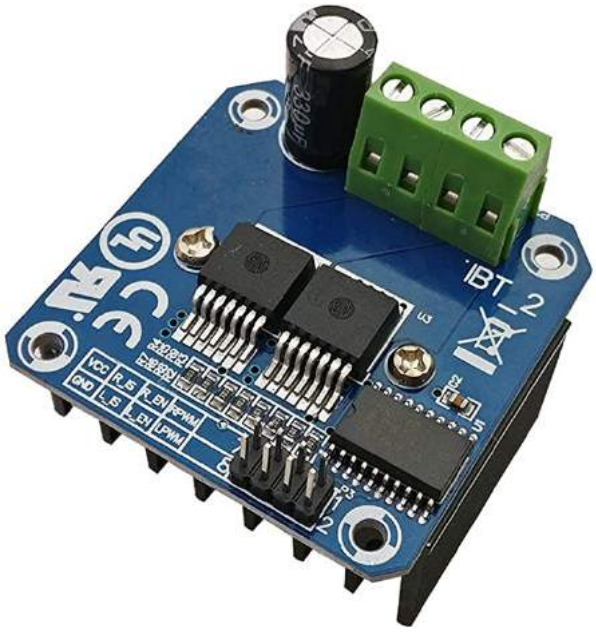

FIGURE 24: BTS7960 motor controller

The third and fourth ones were custom made Mosfet H-Bridge and Relay H-Bridge with a Mosfet. They both a voltage drop of 1.5V and 0.6V from the capacitors to motors, respectively because of the mosfets. The last one and the one we used for competition was a relay H-Bridge which used only relays and did not have any voltage drop at the expense of speed control.

The initial plan was to use the fourth controller, Relay H-Bridge & Mosfet; however, there was not enough time to implement the PID speed cascaded controller with the motor controller. Figure 13 shows the schematic for the fourth motor controller iteration or the Relay H-Bridge with a Mosfet for the PCB.

7.5 Bluetooth Remote Controller

Figure 25 shows the user interface (UI) of the Arduino Bluetooth app. The app was done on MIT App Inventor 2.

FIGURE 25: Phone Bluetooth UI

Figure 26 displays the variables and Bluetooth connection feature of the app. The "Select Device" button allows the user to select which Arduino Bluetooth module they want. The "Disconnect Bluetooth" button allows the user to disconnect any Bluetooth device the phone is currently connecting.

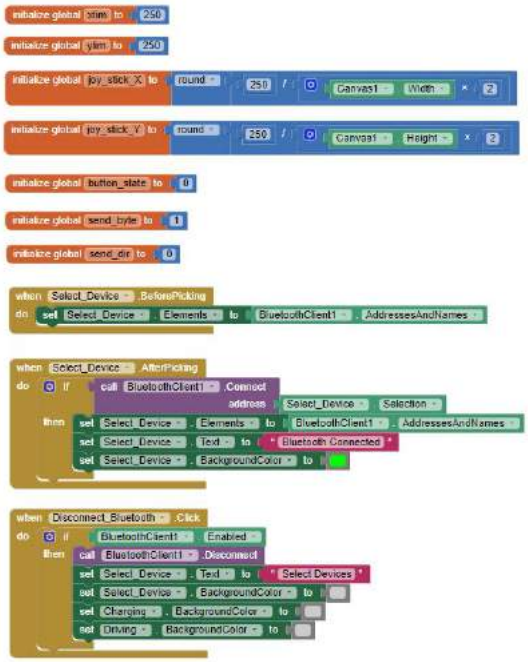

FIGURE 26: Bluetooth Variables and Communication Block Code

Figure 26 displays the charging, driving, and joystick feature of the app. The "Charging" button sends a signal to the Arduino to enable the alternator to start charging the device and disable the device to drive. The "Driving" button sends a signal to the Arduino to enable the device to drive and disable the alternator to charge the device. The black ball or the joystick send a signal to the Arduino on how to drive. If the user drags the joystick up, the

device will drive forward. If the user drags the joystick left, the device will rotate left. If the user drags the joystick right, the device will rotate right. If the user drags the joystick down, the device will drive backward. If the user releases the joystick, then the device will stop.

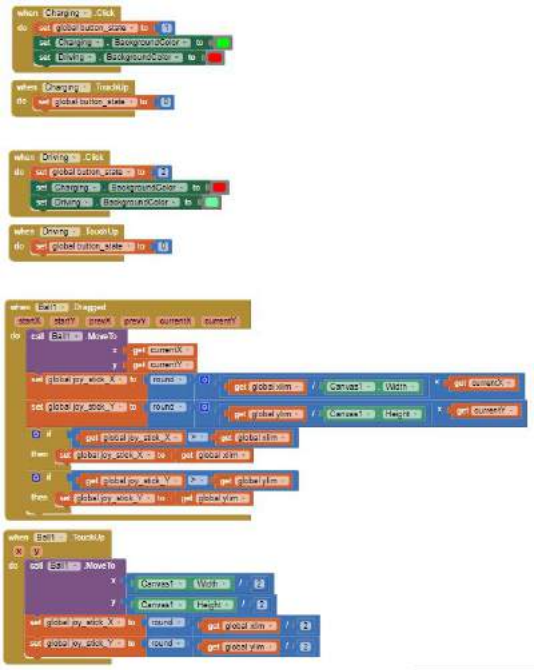

FIGURE 27: Bluetooth Controls Block Code

Figure 28 displays how the information is transmitted to the Arduino in 3 packets. The first packet represents the address of the information for the Arduino to recognize and accept. The second packet represents the information from the "Charging" button or the "Driving" button. The third packet represents the information from the joystick. The app will transmit the information every 20ms.

FIGURE 28: Bluetooth Sending Data Block Code

7.6 Feedback Control

The feedback control diagram that was going to be used is shown in Figure 29.

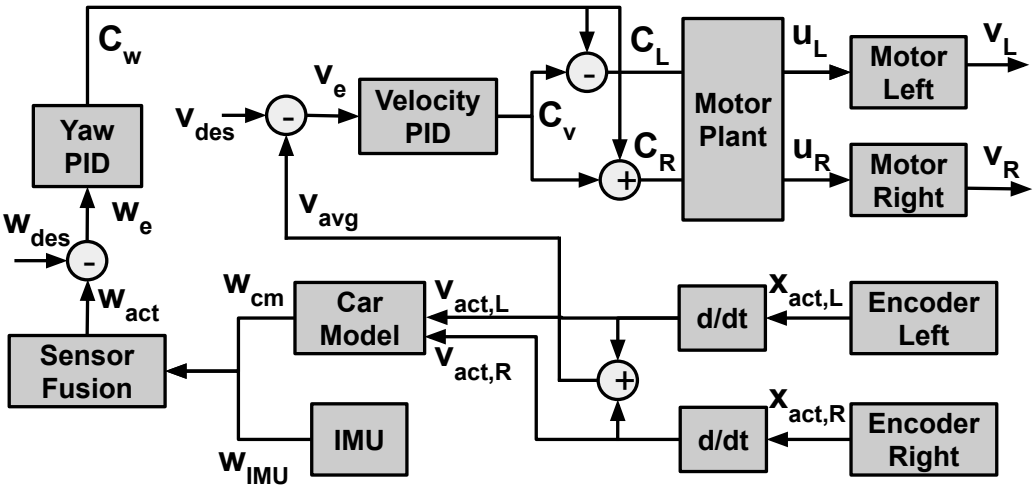

FIGURE 29: PID speed cascaded controller

For controlling the device speed and orientation, we send a desired velocity v_{des} and a desired yaw angle w_{des}. First, the velocity error v_e is taken by the difference between the v_{des} and v_{avg} which is the average velocity calculated from the encoders on the left an right motors. If the device has to turn, then the controller output from the Yaw PID C_w will be added or subtracted to the controller output from the velocity PID C_v, outputting the left controller output C_L and right controller output C_R respectively. Then C_L and C_R will be inputted into the motor plant, creating a saturation signal or voltage u_L and u_R for the left and right motor to receive. The left and right motors output a velocity v_L and right motor velocity v_R, respectively.

There are two ways to calculate the actual yaw angle. The left and right velocity are inputted into a car model which outputs the yaw angle ω_{cm} The car model is defined by the following equation.

$$\omega_{cm} = \frac{(v_R - v_L)L}{2} \tag{86}$$

L is the distance between the two front wheels. The Inertial Measurement Unit (IMU) outputs the yaw angle ω_{IMU} Then ω_{cm} and ω_{IMU} are weighted according into the sensor fusion block which outputs the actual yaw angle w_{act} Finally the yaw angle error ω_e is taken by the difference between the ω_{des} and ω_{avg} and is inputted into the Yaw PID to output C_w.

7.7 Baseplate FEA

Baseplate calculations were performed to ensure it would not deflect too much under the weight of the device and water. For the hand calculations, a simplification was made that showed the distributed load extended the entire length of the baseplate, as shown in Figure 30. The load was compensated to maintain the same pressure per unit length. With the simplification, the baseplate could then be calculated as a simply supported beam under a distributed load, as shown in Figure 31.

The moment of inertia can be calculated for a the rectangular cross-section of the baseplate.

$$I = \frac{1}{12}bh^3 = \frac{1}{12}(0.3\,m)(0.0045\,m)^3 = 2 \times 10^{-9}\,m^4 \tag{87}$$

The deflection can then be calculated. The young's modulus used was the young's modulus listed on Canal Plastics' (the supplier for the acrylic we purchased) in their acrylic physical properties document.[8] The load was assumed to be the device plus $7L$ of water, which is a lot more than it would ever experience.

$$\delta = \frac{5wL^4}{384EI} = \frac{5(196.2\,N/m)(0.38\,m)^4}{384(3300 \times 10^6\,N/m^2)(2 \times 10^{-9}\,m^4)} = 0.0071\,m \tag{88}$$

The deflection was calculated to be only $7.1\,mm$, which was acceptable.

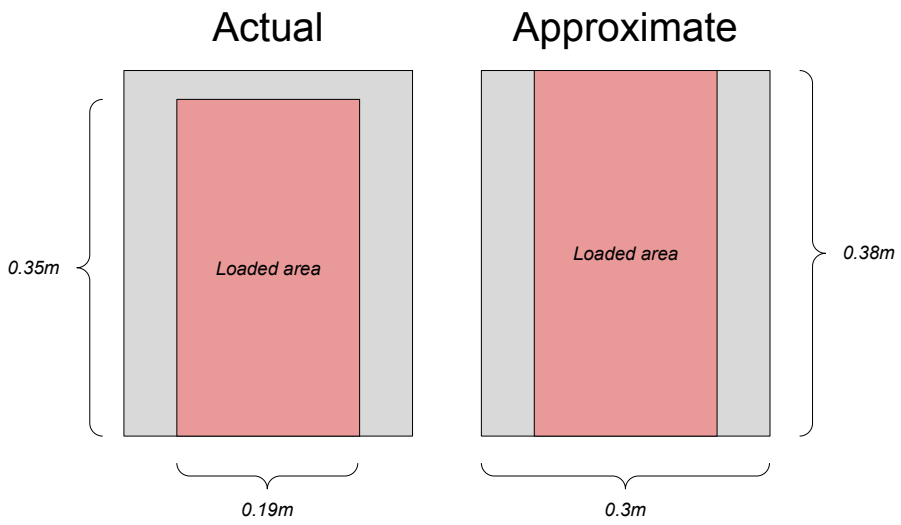

FIGURE 30: The baseplate (drawn to scale) was simplified to have the pressure load over the entire length.

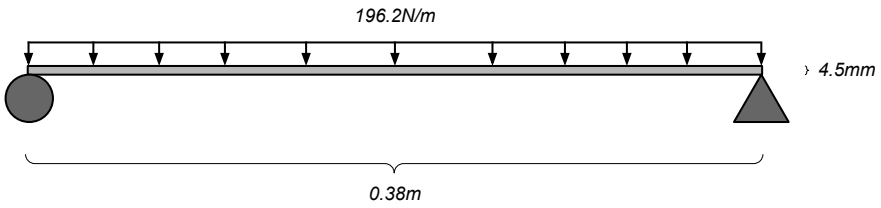

FIGURE 31: Side view (drawn to scale) of the simplified baseplate showing it is a simply supported beam with a distributed load.

An FEA simulation was also performed in ANSYS APDL (see Table 1 for the simulation settings) to get a more accurate deflection value as well as the stress. The hand calculation was in agreement with the simulation (within an order of magnitude), verifying the simulation results. The simulation showed the plate would only deform $2.7\,mm$, which is negligible. Therefore, the baseplate would be able to withstand more than the necessary amount of weight.

Table 1: ANSYS APDL simulation settings

Elements	SOLID185
Young's Modulus	3300 MPa
Dimensions	$0.3\,m \times 0.38\,m \times 0.0045\,m$
Loaded Area Dimensions	$0.19\,m \times 0.35\,m$
Load	$192.6\,N/m^2$
Boundary Conditions	0DOF for the upper left corner (at Z=0) 0DOF for the upper right corner (at Z=0) 0UZ for the lower middle (at Z=0)

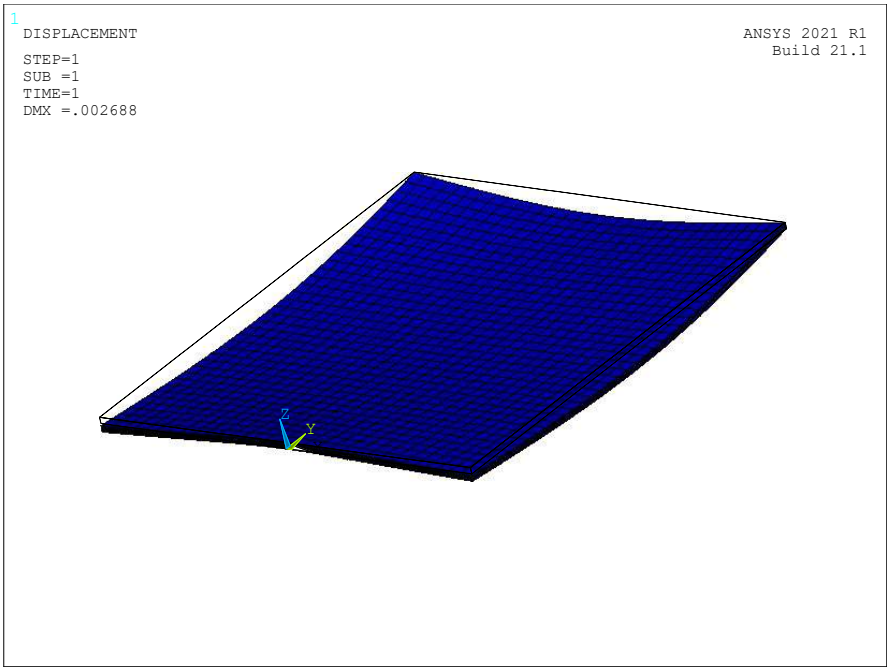

FIGURE 32: The deformed plate with an outline showing the undeformed plate. The deformation is exaggarated to show the movement better.

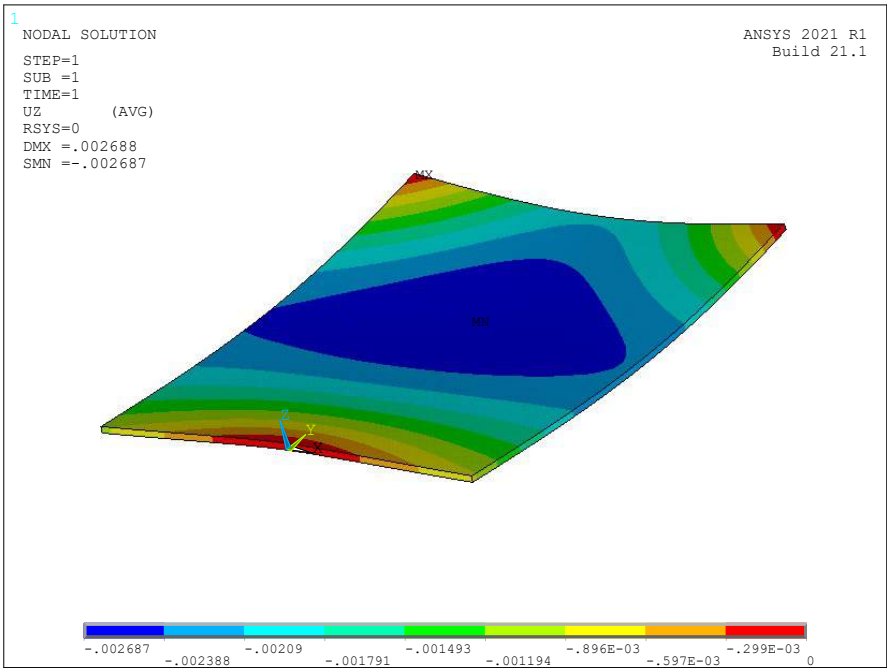

FIGURE 33: The colormap shows the deformation amount at each point. The center deforms the most, but is only $2.7\,mm$ downwards.

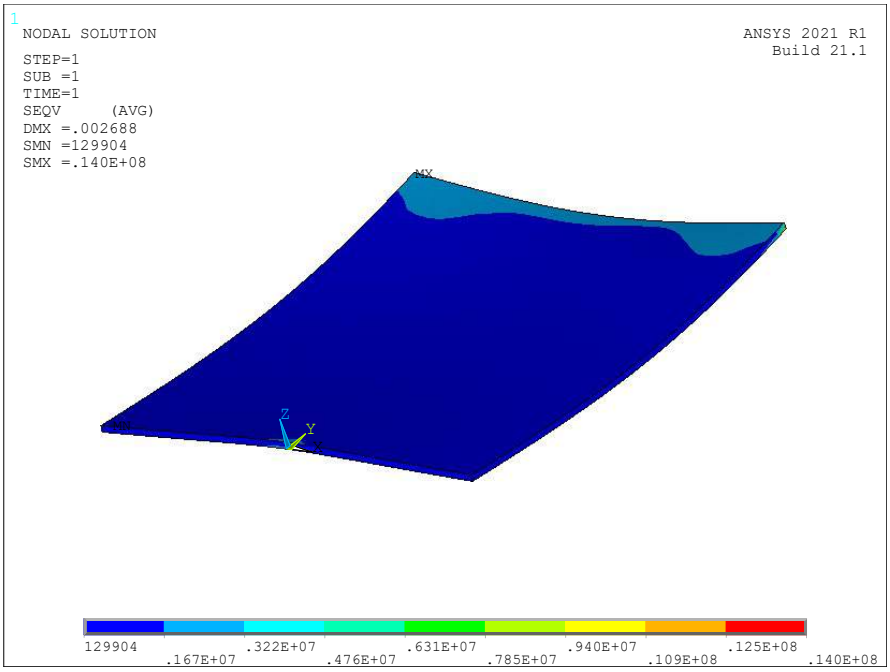

FIGURE 34: The colormap shows the Von Mises stress in the baseplate. The corners show the highest amount of stress, but these are artificial stress concentrations that occurred due to the boundary conditions.

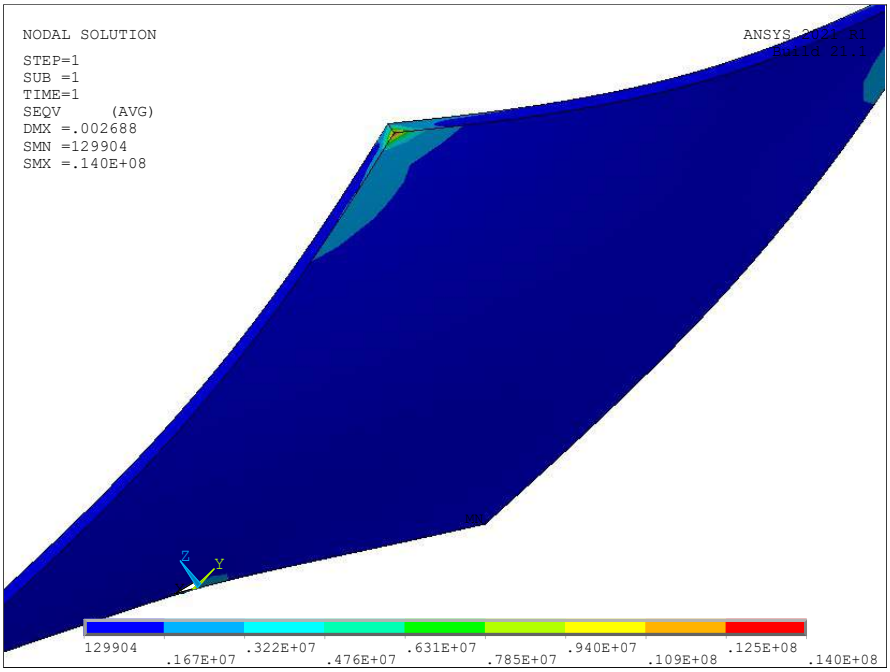

FIGURE 35: A closeup of a corner where the stress concentration occurred. This was a consequence of the boundary conditions.

7.8 Energy Loss Calculations

The energy from the water draining from the bucket, E_{bucket}, can be calculated using the equation

$$E_{\text{bucket}} = \rho g h Q \mathrm{d}t \tag{89}$$

where $\rho = 997\,kg/m^3$ is the density of water, $g = 9.81\,m/s^2$ is gravity, $h = 2.5\,m$ is the height of the bucket from the ground, $Q = 0.375\,L/s$ is the flow rate of the water (this was calculated using a stopwatch and bucket with measurement markings), and $\mathrm{d}t = 4.5\,min$ was the charging time. Plugging those values in gives $E_{\text{bucket}} = 2475.7\,J$.

The energy harvested by the alternator, $E_{\text{alternator}}$, can be calculated based on the amount of energy the Pelton turbine can collect, which can be calculated according to the following equation

$$E_{\text{alternator}} = 2\rho Q(v_{jet} - v_{turbine})v_{turbine}\mathrm{d}t \tag{90}$$

where $v_{jet} = 2.96\,m/s$ is the velocity of the water jet (calculated based on the water flow rate and nozzle cross-sectional area) and $v_{turbine} = 0.721\,m/s$ is the linear velocity of the turbine (calculated based on the angular velocity and turbine diameter). Plugging those values in gives $E_{\text{alternator}} = 326.1\,J$.

According to the theory on Pelton turbines, the ideal linear velocity would be half the jet velocity.[9] If this was achieved, the energy would have been $E_{\text{alternator,ideal}} = 442.3\,J$. Therefore, the turbine was operating at 73.7% of the ideal.

The energy that was stored in the capacitors, $E_{\text{capacitors}}$, can be calculated using the equation

$$E_{\text{capacitors}} = \frac{1}{2}CV^2 \tag{91}$$

where $C = 4\,F$ is the total capacitance and $V = 7.5\,V$ was the charge on the capacitors. Plugging those values in gives $E_{\text{capacitors}} = 112.5\,J$.

The unusable energy, E_{unusable}, was the energy left over in the capacitors. This was calculated the same way as the capacitor energy but with $V = 2.5\,V$ corresponding to the voltage left on the capacitors. Plugging in that value gives $E_{\text{unusable}} = 37.5\,J$. That means that the motors got $E_{\text{motors}} = E_{\text{capacitors}} - E_{\text{unusable}} = 75\,J$.

Lastly, the energy used to move the device, E_{motion}, can simply be approximated as the mechanical energy, calculated using the equation

$$E_{\text{motion}} = \frac{1}{2}mv^2 \tag{92}$$

where $m = 4.4\,kg$ was the mass of the device and $v = 0.314\,m/s$ was the average velocity (calculated by taking the distance traveled and dividing it by the time it took to do so). Plugging those values in gives $E_{\text{motion}} = 0.2\,J$.

The above energy loss calculations were the ones used to create the Sanky diagram shown in Figure 16. They are not exact, but still give a good picture of where the energy went.

7.9 Bill of Materials

Table 2 lists all the materials purchased for this project as well as links to the sources. The only non-purchased items were the 3D printed parts.

Table 2: Bill of Materials

Source	Part	Cost (per)	Qty.	Qty. notes	Cost (total)	Use	Link
McMaster	10-32 0.625in socket head bolts	$12.60	1	1 pack	$12.60	Generator mounting hardware	Link
	10-32 1.25in socket head bolts	$7.59	1	1 pack	$7.59	Turbine to rotor mounting	Link
	#10 washers	$2.40	1	1 pack	$2.40	Generator mounting	Link
	10-32 nuts	$2.08	1	1 pack	$2.08	For clamping the shaft on either end	Link
	Caster	$18.30	1		$18.30	Rear caster for the cart	Link
	3/16in bearings	$3.63	10		$36.30	For a smooth rotor and turbine	Link
	3/16 partially threaded rod	$10.03	1		$10.03	To be used as the shaft for the rotor and turbine	Link
	3/4in Clear PVC tubing	$1.53	25	ft	$38.25	Hose for directing water into our device	Link
	Through-wall pipe fitting	$22.13	2		$44.26	Fits in the bucket and device to act as a tap	Link
	Ball valve	$35.14	1		$35.14	For emptying the device tank	Link
	Plastic barbed 3/4in hose fitting	$0.86	1		$0.86	For connecting the hose to the bucket	Link
	6.25gl Bucket	$10.21	1		$10.21	For holding and dispensing water during the competition	Link
	Hose clamps	$9.50	1	10 pack	$9.50	For connecting the hoses	Link
	Plastic tube	$2.93	1		$2.93	To be used as a spacer between the wall and the pelton wheel	Link
Amazon	Water Container	$33.99	2		$67.98	Holding the water on the device and stopping splashing	Link
	Magnets (weaker)	$23.99	1	20 pack	$23.99	For the rotor	Link
	Magnets (stronger)	$17.99	2	8 packs	$35.98	For the rotor	Link
	Measuring container	$16.56	1		$16.56	Required for measuring each round's points (per rules)	Link
Pololu	Motors	$34.95	2	2 motors	$69.90	For moving the cart	Link
	Wheels	$7.95	1	1 set	$7.95	Front wheels for the cart	Link
	Wheel collets	$6.95	1	1 set	$6.95	Stronger wheel collets to keep the wheels in place	Link
	Motor mounts	$7.45	1	1 set	$7.45	For holding the motors in place	Link
	Mounting screws 14mm M3	$1.29	1	25 pack	$1.29	For connecting the wheels to the collets and the brackets to the base	Link
	Mounting nuts M3	$1.95	1	25 pack	$1.95	For holding the motor brackets	Link
Remington Industries	28 gauge magnet wire	$39.11	1	1, 2.5lbs roll (5068')	$39.11	For the stator coil windings	Link
	Wheels	$5.45	1	1 set of 2	$5.45	Alternative wheels for the universal hub to enable more torque	Link
	IMU	$34.95	1	1 set	$34.95	Accelerometer for cart control	Link
	Motors	$45.95	2	2 motors	$91.90	For moving the cart	Link
Canal Plastics Center	Clear Acrylic	$9.30	2	12"x18"x3/16"	$18.60	For the base platform of the cart	Link